Ab initio calculation of the phonon dispersion in bulk InP and in the InP(110) surface

J. Fritsch, P. Pavone, and U. Schröder
Institut für Theoretische Physik der Universität Regensburg, D-93040 Regensburg, Germany
(Received 11 April 1995)

An *ab initio* linear-response approach based on the density-functional theory has been used to investigate the dynamics of bulk InP and of the InP(110) surface. The plane-wave pseudopotential method together with the slab supercell description for the surface have been employed in order to determine the complete bulk phonon spectrum, the atomic geometry of the InP(110) surface, and the surface phonon dispersion in a consistent formalism. The calculated structural and dynamical properties of both the bulk and the surface compare very well with all available experimental data. Furthermore, we examine the influence of the structural details of InP(110) on the surface vibrational features. Our *ab initio* results indicate the fingerprints of the relaxation geometry in the surface phonon dispersion.

I. INTRODUCTION

Density-functional calculations based on the linear-response formalism proposed by Baroni, Giannozzi, and Testa[1] have proven to be a very efficient method for determining the lattice dynamics in elemental and compound semiconductors. The calculated phonon dispersion curves compare very well with the spectra obtained from inelastic neutron diffraction and Raman scattering.[2] A recent application of *ab initio* linear-response theory to GaAs(110) has shown that also for the surface of a binary semiconductor, the atomic equilibrium positions and the vibrations can be determined within the same formalism, completely consistent with the calculation of the structural and dynamical bulk properties without introducing any adjustable parameters or modifications.[3] The agreement of the calculated surface phonon dispersion with all available experimental data from inelastic scattering of He atoms[4,5] and high-resolution electron-energy-loss spectroscopy[6] (HREELS) is comparable to the accuracy of the *ab initio* results for the bulk phonon spectra.[2] Among all previous theoretical investigations on bulk InP and InP(110), first-principles calculations have been devoted only to the determination of the zone boundary frequencies of the longitudinal bulk phonons at the X point within the frozen-phonon approach[7] and to the examination of the atomic geometry and the electronic states of the (110) surface.[8,9] In the present paper, we have used the density-functional perturbation theory (DFPT) of Baroni and co-workers[1,2] in the extension of Ref. 3, in order to perform an *ab initio* calculation of the complete vibrational spectra for bulk InP and for the InP(110) surface. An application of DFPT to the study of the structure and phase stability of $Ga_xIn_{1-x}P$ solid solutions was presented in Ref. 10.

The bulk phonon dispersion of InP has been measured with high precision by inelastic neutron scattering[11] and by Raman spectroscopy.[12,13] With the exception of Ref. 7, most of the previous theoretical investigations on the lattice vibrations in InP are based on model calculations,[14–17] the results being characterized by an underestimation of the frequency of the LA phonon near the X point and by different predictions for the dispersion of the optical phonons in the Σ direction. The frozen-phonon calculation of Wang, Gu, and Li[7] underestimates the experimentally observed frequencies for InP by about 10%. Lately, HREELS has been used by Nienhaus and Mönch,[18] in order to measure the surface phonon dispersion in InP(110) along the high-symmetry directions parallel and perpendicular to the surface In-P chains. Beside the tight-binding molecular dynamics simulations of Schenter and LaFemina,[17] to our knowledge the only calculations of the phonon dynamics in InP(110) up to now have been done by Das and Allen[19] using a simple force-constant model and by Wang and Duke[20] using a tight-binding model. Hence, there is certainly need for further theoretical investigations based on *ab initio* calculations.

The surface geometry of InP(110) has been investigated by low-energy electron diffraction (LEED),[21–23] x-ray standing-wave (XSW) measurements,[24] and by the combination of the XSW method with extended x-ray-absorption fine structure (EXAFS).[25] Very recently, the structure of InP(110) has been examined with the help of polarization-dependent photoemission EXAFS[26] and by low-energy positron diffraction.[27] The relaxation of InP(110) is very similar to the atomic structure of the (110) surfaces of most of the III-V compounds.[9,28,29] It is characterized by an inward relaxation of the group-III surface atoms, while the group-V first-layer atoms are shifted above the surface. This leads to a nearly bond-length-conserving rotation of the surface chains by a tilt angle of about 25°–30° depending on the particular compound. The driving mechanism of the atomic rearrangement arises from the fact that the first-layer anions prefer a p-bonding configuration with their group-III neighbors, which lowers the energy of the occupied dangling bonds at the surface, while the first-layer cations prefer to be situated in a more sp^2-like bonding configuration with their group-V neighbors, which increases the energy of the un-

0163-1829/95/52(15)/11326(9)/$06.00

occupied surface dangling bonds. In order to achieve a correct description of the surface vibrations, it is necessary to determine self-consistently the atomic equilibrium positions, the electronic structure of the relaxed surface, and the charge redistribution related to atomic displacements.

In the present paper we report the results of our *ab initio* calculations for the bulk phonon dispersion of InP as well as for the structural and vibrational properties of the InP(110) surface. A brief summary of the details of the plane-wave density-functional perturbation scheme, which is the basis of all of our calculations, is given in Sec. II. In Sec. III, we show our results for the bulk phonon dispersion of InP. We compare the phonon dispersion with previous theoretical investigations and experimental data from inelastic neutron diffraction and Raman spectroscopy. The calculated structural and dynamical properties of InP(110) are presented in Sec. IV including a comparison with the results from various experiments[18,21–23,27] and theoretical investigations.[8,9,19] The subsequent discussion of the most prominent surface-localized modes in Sec. V is focused on the dependence of the surface vibrations on the atomic structure of InP(110).

II. THEORETICAL FRAMEWORK

Our calculations are carried out within the density-functional theory together with the local-density approximation.[30,31] For the exchange-correlation potential we use the form of Ceperley and Alder[32] in the parametrization of Perdew and Zunger.[33] To describe the electron-ion interaction, we use the norm-conserving nonlocal pseudopotentials already applied in Ref. 10. The electronic wave functions are expanded in plane waves up to a maximal cutoff energy of 16 Ry for the bulk and 10 Ry for the surface calculations. In order to check the reliability of our results, further calculations have been performed on the basis of additionally constructed pseudopotentials for indium and phosphorus.[34,35]

The bulk is described in the zinc-blende symmetry. To extend the plane-wave formalism to the (110) surface of a III-V semiconductor, we introduce periodically repeated thin crystal films fixing the lattice constant at the theoretical value determined for the bulk. Each slab spans nine atomic layers, two neighboring slabs are separated by a vacuum spacing which is equal to three removed atomic (110) layers. Such a distance between two neighboring slabs turned out to be large enough, as the electronic band structure remained unaffected irrespective of an increase in the size of the vacuum region. Further evidence is provided by a phonon calculation performed for GaAs(110), which has shown no dispersion perpendicular to the slabs.[3] The number of atomic layers per crystal film guarantees that also the surfaces bordering one slab are sufficiently decoupled. For the **k**-point sampling, we use ten special points in the irreducible wedge of the Brillouin zone of the zinc-blende structure and six special points in the irreducible part of the surface Brillouin zone for the repeated slab configuration.

The bulk lattice constant a_0 has been determined by fitting the Murnaghan equation of state[36] to a discrete set of total energies $E(a)$ calculated for various values of the lattice parameter a. The atomic ground-state configuration of InP(110) is found by minimizing the total energy with the help of the Hellmann-Feynman forces starting the atomic relaxation from a configuration derived from the equilibrium geometry of the GaAs(110) surface.[3] Each atom was allowed to move. The translational degrees of freedom are suppressed by fixing the center of mass of the two central layer atoms in the slab supercell at the corresponding bulk position. The equilibrium positions are defined with a numerical uncertainty of less than 0.01 Å when all forces are smaller than 0.1 mRy/a.u.

The phonon dispersion of the bulk has been determined by means of the DFPT of Baroni and co-workers.[1,2] The details of our calculation are exactly the same as those described in Ref. 2. Within the DFPT, the second-order derivatives of the total energy such as the dynamical matrices are calculated from the static linear response of the electrons to the variation of the external potential corresponding to periodic displacements of the atoms. The response of the electrons is calculated iteratively, until self-consistency is achieved between the variation of the charge density and the screened perturbing potential. In order to determine the complete bulk phonon dispersion of InP, we calculate the dynamical matrices at a grid of eight uniformly distributed points corresponding to a (444) mesh for the zinc-blende structure.[37] The dynamical matrices at arbitrary wave vectors can be evaluated with the help of a Fourier deconvolution on this mesh.

For a proper description of the force constants at the surface, it is important to treat self-consistently the charge redistribution induced by a lattice distortion taking fully into account the presence of the surface with its particular atomic and electronic properties. This is accomplished by applying the DFPT also to the periodic configuration of the fully relaxed nine-layer slabs. We calculate the dynamical matrices of the thin crystal films at four points in the $\overline{\Gamma X}$ and three points in the $\overline{\Gamma X'}$ direction of the surface Brillouin zone.

III. BULK PHONON SPECTRUM

All of the results presented in this and in the following section have been obtained by using the same pseudopotentials as in Ref. 10. We have determined the bulk lattice constant a_0 for various cutoff energies. At 16 Ry, we obtain $a_0 = 5.805$ Å in good agreement with $a_0 = 5.870$ Å measured at 16 °C.[38] As the lattice constant has been calculated at $T = 0$ neglecting the effects of the zero-point motion, our result should be compared with the corresponding value of $a_0 = 5.858$ Å estimated from the extrapolation of the experimental data given in Ref. 38 to zero temperature. The remaining slight underestimation by about 1% is typical for LDA calculations. Our lattice parameter is somewhat higher than obtained from previous calculations.[9] This discrepancy of the theoretical results can be attributed to the different pseudopoten-

tials used in Ref. 9.

Already at 10 Ry sufficient accuracy is achieved in the calculated values for the lattice constant, the bulk modulus, and also the bulk phonon frequencies. This is essential for our surface calculations, which have been accomplished by using plane waves up to 10 Ry for the expansion of the electronic states. As can be seen from Table I, no significant changes occur for an increase in the cutoff energy up to 16 Ry for which all of the bulk properties are converged. With the exception of the transverse optic branches, the changes in the frequencies are negligible. The transverse optic phonon branches are shifted slightly upwards by about 0.1–0.2 THz without any significant variation of the dispersion increasing the cutoff energy from 10 to 16 Ry.

The temperature dependence of the phonon energies can be estimated from the variation of the Γ point frequencies in Raman spectroscopy performed at 4 and 300 K.[12,13] At room temperature, the optic Γ point phonons are shifted downwards by about 0.15 THz with respect to low temperatures. For a comparison of the scattering data mainly obtained from inelastic neutron diffraction at room temperature we should bear this in mind. Figure 1 summarizes our results for the phonon dispersion curves along various directions of high and low symmetry together with the neutron-scattering data of Borcherds *et al.*[11] and the frequencies determined in Raman spectroscopy.[13] The calculated phonon frequencies compare very well with the experimental data measured along the Δ, Σ, and Λ direction. In the other directions, for which no experimental data are available, our parameter-free *ab initio* calculation provides reliable predictions for the phonon dispersion curves.

Because of the large mass mismatch between indium and phosphorus, the optic branches are very flat. As a result not only the acoustical and optical phonons are separated by a gap (from 5.62 to 9.15 THz) but also the transverse optic and longitudinal optic phonon branches (from 9.81 to 10.02 THz), as can be seen from the dispersion curves and from the density of state shown in Fig. 2. While the model calculations of Refs. 14 and 15

TABLE I. Lattice constant a_0 (in Å), bulk modulus B_0 (in Kbar), and optic phonon frequencies (in THz) calculated at 10 and 16 Ry in comparison with experimental results from x-ray diffraction, coherent inelastic neutron scattering, and from Raman scattering. The experimental data are taken from Refs. 11, 13, and 38. The theoretical values correspond to zero temperature. Experimental data obtained at room temperature are indicated by (RT).

	10 Ry	16 Ry	Exp.
a_0	5.822	5.805	5.870 (RT)
B_0	711	736	710 (RT)
$\nu_{TO}(\Gamma)$	9.34	9.52	9.24 (4 K)
$\nu_{LO}(\Gamma)$	10.59	10.61	10.48 (4 K)
$\nu_{TO}(X)$	9.65	9.73	9.70 (RT)
$\nu_{LO}(X)$	10.00	10.02	9.95 (RT)
$\nu_{TO}(L)$	9.45	9.58	9.50 (RT)
$\nu_{LO}(L)$	10.14	10.15	10.23 (RT)

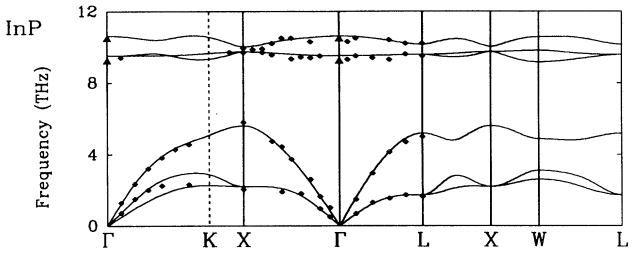

FIG. 1. Phonon dispersion of InP calculated with a cutoff energy of 16 Ry in comparison with the neutron-diffraction data of Ref. 11 (diamonds) and the results of the Raman experiment of Ref. 13 (triangles).

predict two gaps in accordance to our findings, the phenomenological parameter model of Kagaya and Soma[16] suggests a completely different dispersion in the optic region with significant deviations from the measured frequencies. The existence of a gap in the bulk band structure is interesting, especially if the formation of a surface will lead to a phonon band lying in the gap region. Such an additionally appearing branch could be identified unambiguously as the band of a surface-localized phonon. Like in Refs. 14 and 15 the flatness of the transverse acoustic branches is well reproduced in our calculation. For the optic phonon dispersion in the (110) direction, only small differences occur between our predictions and those of the model calculations. However, the frequencies of the longitudinal acoustic zone boundary phonons are underestimated to a larger extent in Refs. 14 and 15 as well as by the first-principles frozen-phonon approach of Wang, Gu, and Li.[7]

As the parameters of the model calculations are optimized, in order to reproduce only the bulk phonon spectra, further assumptions and adjustments would be necessary for a proper description of the variation of the force constants at a surface, due to the relaxation and the electronic charge redistribution. Within the density-functional linear-response approach, however, the static and dynamical properties of a semiconductor surface can be obtained in one consistent formalism together with the bulk phonons without introducing any modifications.

IV. THE InP(110) SURFACE

In order to find the atomic ground-state geometry, we minimize the total energy with the help of the Hellmann-

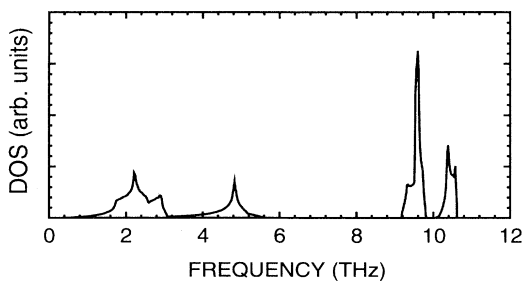

FIG. 2. One phonon density of state in InP calculated at 16 Ry.

TABLE II. Surface relaxation of InP(110) in comparison with previous pseudopotential calculations (Refs. 8 and 9) and with experimental data from low-energy positron diffraction (Ref. 27) and LEED (Refs. 21–23 and 27). The structural parameters $\Delta_{1,\perp}$, $\Delta_{1,\parallel}$, $\Delta_{2,\perp}$, $d_{12,\perp}$, $d_{12,\parallel}$, and ω are defined in Fig. 3.

	Present	Umerski and Strivastava Ref. 8	Alves *et al.* Ref. 9	Chen *et al.* Ref. 27		Ford *et al.* Ref. 21	Duke *et al.* Ref. 22	Meyer *et al.* Ref. 23
$\Delta_{1,\perp}$ (Å)	0.636	0.60	0.670	0.605	0.752		0.730	0.690
$\Delta_{1,\parallel}$ (Å)	4.602		4.517				4.598	4.691
$\Delta_{2,\perp}$ (Å)	0.106	0.079	0.117	0.077	0.055		0.140	0.068
$d_{12,\perp}$ (Å)	1.548	1.511	1.435				1.549	1.411
$d_{12,\parallel}$ (Å)	3.321		3.216				3.382	3.450
ω (deg)	27.5	27.1	30.1	24.3	32.0	31.1	29.9	30.4

Feynman forces. The positions of all of the atoms in the slab are varied by means of a modified Broyden scheme[39] until all forces are smaller than 0.1 mRy/a.u. At this stage the theoretically determined equilibrium positions are defined with a numerical accuracy of ±0.01 Å. The central-layer atoms, which also were allowed to relax, remain in their bulk positions. Table II summarizes our results for the surface relaxation including a comparison with the data obtained from the pseudopotential calculations of Refs. 8 and 9, from LEED experiments[21,23,27] and low-energy positron diffraction.[27] The structural parameters are defined in Fig. 3.

The first-layer anions are lifted above the surface by 0.211 Å, while the uppermost In ions are shifted below the surface by 0.425 Å. In good accordance with recent results from LEED measurements,[21,27] EXAFS studies,[26] and low-energy positron diffraction,[27] the variation in the bond lengths is very small compared to the atomic displacements. Therefore, the surface relaxation essentially consists in a nearly bond-length-conserving rotation of the surface chains leading to a buckling angle of about 27.5° and a slight counter-rotation in the second layer by about 4.1°, in good agreement with the *ab initio* results of Umerski and Srivastava.[8] In their equilibrium positions, the first-layer anions are situated in a pyramidal configuration, while the surface cations are bonded to their nearest neighbors in a nearly planar sp^2 configuration. This has a strong influence on the force constants at the surface. The appearance of surface-localized modes that are closely related to this relaxation should be an indication of the atomic geometry. The frequency of such phonon modes could give an estimation for the magnitude of the tilt angle. (See the discussion in the subsequent section.)

The surface phonon calculation has been accomplished by calculating the dynamical matrices of a periodic configuration of fully relaxed nine-layer slabs with the help of the DFPT. We find that the force constants of the two outermost layers in the thin crystal films are significantly different from the corresponding bulk values, while the central layers are bulklike.

In order to identify resonances and deeply penetrating surface states, we construct the dynamical matrices of larger slabs comprising 25 atomic layers. The force constants in the surface regions of the large crystal films are assumed to be the same as the respective force constants in the nine-layer slabs. For the inner region of the large crystal films, we simply use the bulk force constants without any modifications. We construct four dynamical matrices in the $\overline{\Gamma X}$ direction and three dynamical matrices in the $\overline{\Gamma X'}$ direction. The full dispersion parallel and perpendicular to the surface chains has been obtained by means of a one-dimensional Fourier deconvolution of these matrices.

Figure 4 summarizes our results including a comparison with the experimental data of the HREELS analysis of Nienhaus and Mönch.[18] As already mentioned in Sec. III, there are two gaps in the surface-projected bulk band structure, which is represented by the shaded areas. In the following part we describe, in ascending order of the energy, the surface-localized features identified in our theoretical investigations. In order to compare our results with the experimental data of Ref. 18, we specify the energies of the surface vibrations in meV in contrast with the bulk phonon frequencies, which are usually given in THz (1 THz = 4.141 meV).

The lowest modes in both directions are similar to those found for GaAs(110).[3] In the $\overline{\Gamma X}$ direction the two acoustic phonon branches, which are also resolved

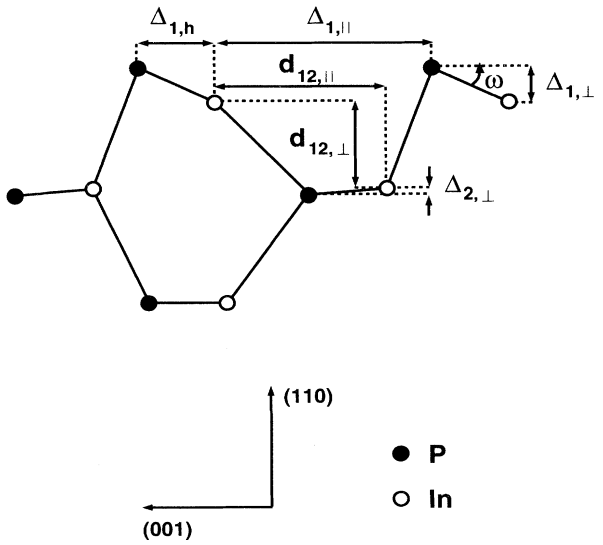

FIG. 3. Relaxation of the InP(110) surface illustrated by a side view of the first three layers. The relaxation parameters refer to Table II.

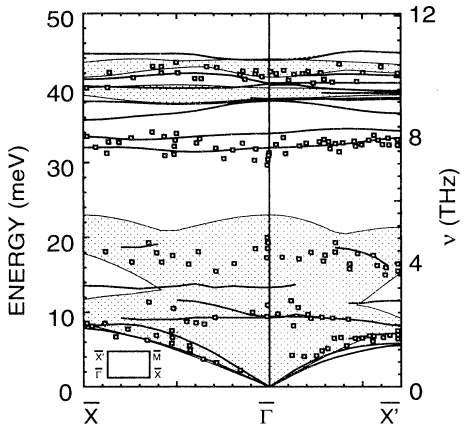

FIG. 4. Dispersion of the localized phonon modes in the relaxed InP(110) surface (solid lines) calculated at a cutoff energy of 10 Ry in comparison with the results of the HREELS measurements of Ref. 18 (squares). The shaded areas represent the surface projected bulk band structure. The inset illustrates the irreducible wedge of the surface Brillouin zone.

in the HREELS measurements,[18] are the Rayleigh wave (RW), which is characterized by in phase displacements in the (110) direction near the $\overline{\Gamma}$ point, and a second mode with pure shear horizontal polarization for small wave vectors. At the $\overline{X}$ point the RW turns into a vibration of the first-layer anions and the second-layer cations perpendicular to the chain direction with larger components normal to the surface and a zone boundary energy of 7.90 meV. Figure 5 illustrates that the second acoustic phonon is complementary to the RW. Approaching the $\overline{X}$ point with an energy of 8.14 meV, it is characterized by a motion of the surface In atoms and the second-layer P atoms mainly normal to the (110) plane, while the anions of the first layer vibrate in the chain direction.

Following the dispersion perpendicular to the surface chains (in the $\overline{\Gamma X'}$ direction), we observe three acoustic surface-localized phonons with the zone boundary energies of 5.56, 5.82, and 7.15 meV. In the $\overline{\Gamma X'}$ direction, no reduction of the symmetry occurs with respect to the $\overline{\Gamma}$ point, so that the slab modes are strictly separated in shear horizontal (SH) modes polarized only in the chain direction and sagittally polarized modes with nonvanishing displacements only in the plane defined by the direction of the wave vector and the surface normal. The intermediate acoustic phonon (5.82 meV) is a pure SH mode, while the other two branches are related to atomic motions perpendicular to the surface chains. At the $\overline{\Gamma}$ point, the RW starts with a displacement pattern normal to the surface, changing its character in the near of the zone boundary to a vibration of the top-layer atoms mainly parallel to the surface and the second-layer atoms perpendicular to the (110) plane. The third acoustic phonon mode exhibits a complementary displacement pattern, as can be seen from Fig. 6. In contrast with GaAs(110), we can resolve the dispersion of this branch for the InP(110) surface only in the vicinity of the $\overline{X'}$ point, as the mode strongly mixes with bulk states.

Starting from the $\overline{\Gamma}$ point in both directions, we ob-

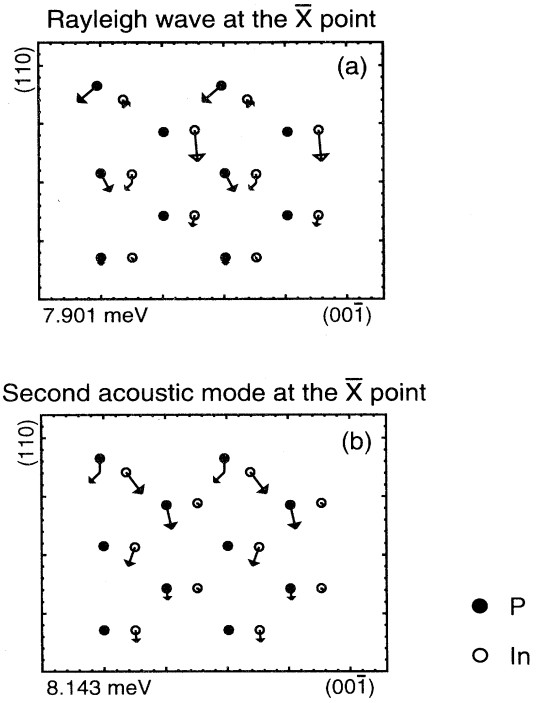

FIG. 5. Displacement pattern of the Rayleigh wave (a) and the second acoustic surface phonon (b) at the $\overline{X}$ point in a side view of the first five layers. The indium atoms are presented by open circles; closed circles refer to the phosphorus atoms. The directions (110) and (00$\bar{1}$) correspond to Fig. 3. Atomic displacements in the chain direction are depicted by arrows with a kink.

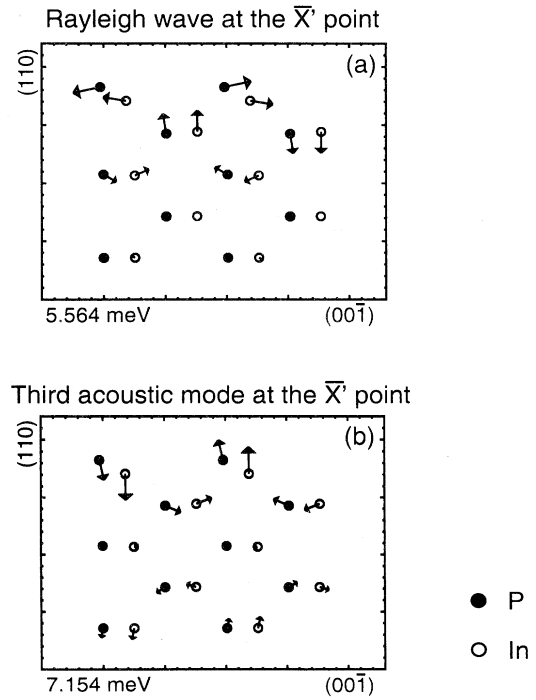

FIG. 6. Same as Fig. 5 but for the eigenvectors of the Rayleigh wave (a) and the third acoustic surface phonon (b) at the $\overline{X'}$ point.

serve the flat branch of a phonon mode at about 9 meV with atomic displacements in the outermost three layers parallel to the surface chains. Near the zone center we can identify a second mode in the same energy range, which is characterized by a rocking motion of the atoms in the surface region penetrating deeply into the crystal film. This mode may have the interpretation of the dynamical version of the surface relaxation. The rocking mode compares to the bond-length-conserving rotations of the top-layer atoms predicted by the tight-binding calculation of Wang and Duke[20] for InP(110) at 7.8 meV and for the (110) surfaces of many other zinc-blende-compound semiconductors in the range 5–14 meV. A similar feature occurs also in GaAs(110).[19] This mode has been expected to couple only weakly to the atomic motions in the deeper layers.[20] In Ref. 3, however, we have pointed out that we could not identify any well defined surface state, which would explain entirely the A_1 mode of the He-scattering experiment of Harten and Toennies.[4] Also in the case of InP(110), we find that the rocking mode strongly mixes with bulk states and cannot be resolved throughout the surface Brillouin zone.

In the energy range between 11 and 14 meV two further modes appear, which can be related to the surface vibrations in GaAs(110). At the $\overline{X}$ point, the mode at 13.58 meV shows a displacement pattern, which is very similar to that of the mode denoted as A_2 in the case of GaAs(110).[3] It is characterized by a motion of the first-layer anions in the plane defined by the topmost anions and their nearest neighbors in the surface layer, while the topmost cations vibrate in the chain direction. The eigenvector of the 11.55-meV feature at the $\overline{X'}$ point shows a similar behavior in the atomic motion of the anions but it is different with respect to the displacements of the cations (Fig. 8). Below the upper edge of the projected acoustic bulk phonon dispersion, we can identify some resonances in the regions indicated by the two short lines between the $\overline{\Gamma}$ and the $\overline{X}$ point and the $\overline{\Gamma}$ and the $\overline{X'}$ point, respectively.

The probably most significant phonons of the InP(110) surface are placed in the gap between the acoustic and optic bulk bands. The vibrational feature measured at about 33 meV is related to a pair of localized modes, which can be extracted from our results in the same energy range, in very good agreement with the experiment. Also the simple two parameter force-constant model of Das and Allen[19] predicts two surface-localized states in the gap, although at about 23 and 29 meV. In the tight-binding molecular dynamics simulations of Schenter and LaFemina two gap modes are seen at 26.7 and 28.1 meV.[17] The eigenvectors of our calculation, representatively shown for the displacements at the $\overline{\Gamma}$ point in Fig. 7, are dominated by a vibration of the first-layer anions. Some similarities of the mode at 33.90 meV to the phonon at 23 meV in GaAs(110) (Refs. 3 and 6) can be recognized. In GaAs(110), however, the vibration is not restricted to solely the first-layer anions. Therefore and because of the large mass ratio between In and P, a direct comparison is not possible. This is also the case for the spectral region of the transverse optical bulk phonons, where a large variety of modes localized in the

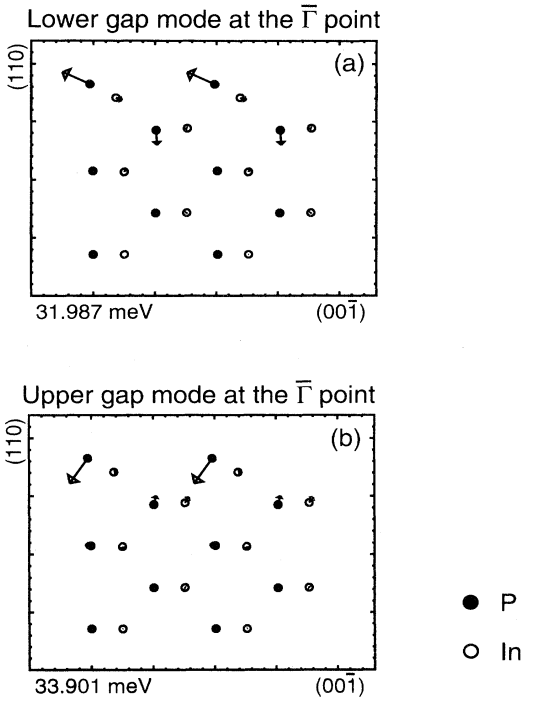

FIG. 7. Same as Fig. 5 but for the eigenvectors of the gap modes at the $\overline{\Gamma}$ point corresponding to the experimentally determined feature at about 33 meV.

first three layers appears in accordance to our results for GaAs(110).

A characteristic feature prominent in InP(110) as well as in GaAs(110) is the surface optical phonon mode situated above the bulk bands. The zone boundary energies are 44.60 meV at the $\overline{X}$ point and 44.75 meV at the $\overline{X'}$ point, respectively. Approaching the $\overline{\Gamma}$ point, it touches the continuum with an energy of 43.76 meV. For the $\overline{\Gamma X'}$ direction, we observe a small LO-TO splitting between the two individual states of the pair related to the surface phonon. Near the zone center the higher mode becomes macroscopic and matches the Fuchs-Kliewer phonon at the bulk phonon edge with an energy of 43.86 meV. The eigenvector of this high-frequency surface optical phonon mode, which is characteristic also for GaAs(110),[3,6,40] is shown in Fig. 8. It is dominated by a motion of the second-layer P ions perpendicular to the chain direction nearly parallel to the (110) plane. In GaAs the character of this mode has been determined to be a predominantly back-bond-like vibration of the first-layer cations against the second-layer anions.

The HREELS experiment of Nienhaus and Mönch resolves the Fuchs-Kliewer phonon at an energy of about 42.3 meV. As the measurements have been performed at room temperature, we have to take into account, as pointed out in Sec. III, that an increase in the temperature from 4 K to 300 K lowers the frequency of the optical zone center phonons of the bulk by about 0.15 THz (≈ 0.6 meV). By using $\nu_{\mathrm{LO}}(300\ \mathrm{K}) = 10.34$ THz and $\nu_{\mathrm{TO}}(300\ \mathrm{K}) = 9.10$ THz for the Γ point frequencies and $\varepsilon = 9.61$ for the dielectric constant (Ref. 38), we obtain $\nu_{\mathrm{FK}}(300\ \mathrm{K}) = 10.23$ THz (≈ 42.4 meV) for the frequency of the

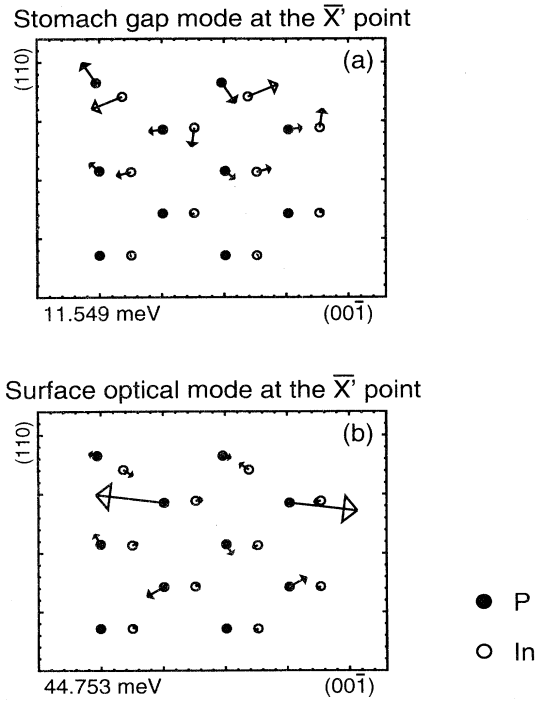

FIG. 8. Same as Fig. 5 but for the eigenvectors of the stomach gap mode at 11.549 meV (a) and the high-frequency surface optic phonon (b) at the $\overline{X'}$ point.

Fuchs-Kliewer phonon, in good agreement with the data from HREELS.[18,41,42]

V. DISCUSSION

In this section we focus on the dependence of the most prominent surface-localized phonon modes on the structural particularities of InP(110). In order to check the reliability of our results presented in Secs. III and IV obtained with the pseudopotentials of Ref. 10 (PP1), we have performed further calculations by using additionally constructed pseudopotentials (PP2),[34,35] for which a cutoff energy of 9 Ry turned out to be sufficiently large to achieve convergency. The comparison of the results obtained from both sets of potentials gives an estimation for the degree of convergence and accuracy of our calculations. Beside the phonon calculation for the bulk and the relaxed surface at high-symmetry points, we have investigated the dynamics of the ideal, unreconstructed surface.

The 9 Ry (PP2) calculation essentially reproduces our results for the bulk obtained with the previously used pseudopotentials PP1. For the lattice constant we obtain $a_0 = 5.800$ Å, which compares very well with the results of Sec. III. In contrast with the longitudinal acoustic phonons, for which the differences are negligible, we note that the frequencies of the transverse acoustic and of the optic phonons are about 0.05–0.10 THz lower in frequency with respect to the 10 Ry (PP1) calculation. The same behavior is expected for the surface vibrations originating in the transverse acoustic and the optic bulk bands.

For the determination of the structural and dynamical properties of the InP(110) surface, we have used the periodic slab configuration of Sec. IV fixing the lattice constant for the 9-Ry calculation, at 5.800 Å. The relaxation parameters obtained from the potentials PP2 agree very well with the results presented in Sec. IV. Only small differences occur in the buckling angle and the other quantities defined in Fig. 3. In the 9-Ry calculation, we find $\omega = 29.1°$ for the surface tilt angle, which is about 1.5° larger compared to $\omega = 27.5°$ determined with the previously used pseudopotentials at 10 Ry. The small differences can be used to analyze the dependence of the surface phonon modes on the microscopic structure of InP(110). Therefore, we have repeated the phonon calculation at the $\overline{\Gamma}$, $\overline{X}$, and $\overline{X'}$ point of the surface Brillouin zone of a fully relaxed periodic slab configuration.

The surface-localized phonon modes identified in this calculation are depicted as open circles in Fig. 9. The frequencies and also the eigenvectors compare very well with our results obtained in Sec. IV using the potentials PP1. Only small changes have to be figured out. Most of the surface-localized features are about 0.4 meV (≈ 0.1 THz) lower in energy in accordance with the behavior found for the transverse acoustical and the optic bulk phonons. For the branches at 11–14 meV, however, both calculations yield nearly the same frequencies in agreement with the findings for the longitudinal acoustic bulk phonon band. Therefore, we conclude that the flat branches placed between 11 and 14 meV originate in the longitudinal acoustic bulk phonons, while the other surface phonon bands below 11 meV are related to the transverse acoustic bulk bands.

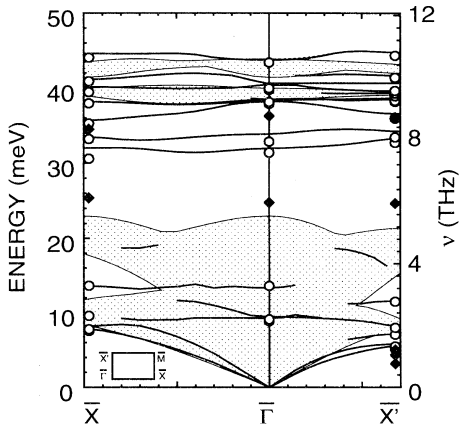

FIG. 9. Surface phonon dispersion of InP(110) calculated with the pseudopotentials PP1 and a cutoff energy of 10 Ry (solid lines) in comparison with the results obtained from the additionally constructed pseudopotentials PP2 and a cutoff energy of 9 Ry (dots and diamonds). The dots refer to the results for the relaxed surface, diamonds indicate the most significant changes occurring at the ideal surface. The shaded areas represent the surface-projected bulk band structure. The inset illustrates the irreducible wedge of the surface Brillouin zone.

Due to the displacement pattern depicted in Fig. 7, one may expect that the two gap modes at about 33 meV are very sensitive even to small variations in the details of the surface structure. As can be seen from Fig. 9, the differences in the frequencies between the 9-Ry and the 10-Ry calculation are larger with respect to all other surface phonon modes. Furthermore, we observe a distinct variation in the eigenvectors for the 9-Ry results, due to an intermixing between the two surface states, which is larger compared to that found in the previous calculation. Hence, the vibrational feature experimentally determined at about 33 meV may be regarded as a real fingerprint of the relaxation. Moreover, a precise measurement of the dispersion of the two surface-localized phonon modes would provide a good estimation for the magnitude of the buckling angle of the surface chains.

In order to demonstrate that the measurement of the surface phonon dispersion of InP(110) unambiguously provides several indications for the relaxation geometry, we have additionally determined the dynamical matrices at the $\overline{\Gamma}$, $\overline{X}$, and $\overline{X'}$ point for the ideal surface. The calculations have been accomplished by using completely unrelaxed nine-layer slabs and the potentials PP2. In the comparison with the results of the relaxed structure the majority of the surface-localized modes shows significant deviations in the frequencies and the displacement patterns.

In Fig. 9 the most important changes imposed by the artificial removal of the relaxation are depicted in the form of diamonds. Supposing the ideal surface, the gap modes are separated by at least 9 meV in contrast with the relaxed structure, for which the splitting essentially is smaller than 2 meV. Because of the large energetical separation, the two phonon branches are completely decoupled. As a consequence, only small modifications in the eigenvectors occur following the dispersion of each of the two modes throughout the surface Brillouin zone. The lower phonon located at about 25 meV is dominated by a vibration of the surface anions in a direction that is similar to the polarization of the mode labeled as (a) in Fig. 7. For the upper mode at about 36 meV, we observe a displacement pattern in accordance to the eigenvector (b) of Fig. 7. The large splitting places the two branches far apart from the feature resolved by HREELS. Hence, the agreement between the experiment and our results for the relaxed surface clearly shows, that the measurement of the gap modes not only is an indication of the buckling of the surface chains but also confirms the range of the tilt angle determined in our calculations.

Another fingerprint of the atomic surface geometry identified in our calculations is the dispersion of the acoustical phonons in the $\overline{\Gamma X'}$ direction. With respect to the relaxed surface, the frequencies of the RW and the third acoustic branch drop down by 2 meV when switching to the unrelaxed system. The eigenvectors of these two modes and also that of the intermediate branch, which is lowered by only 1 meV, remain nearly unaffected. Thus, the displacement patterns shown in Fig. 6 are representative for the ideal surface, too. As the HREELS experiment resolves the surface acoustical phonon above the intermediate branch, the decrease in the frequency at the zone boundary induced by removing the relaxation is a strong indication of the buckling of the In-P chains in the first atomic layer. Therefore, a precise measurement of the dispersion and particularly of the phonon frequencies at the $\overline{X'}$ point should provide additional information about the structural details of InP(110).

Two further remarkable modifications in the vibrational properties can be found. The optical surface phonon, typically placed above the bulk phonon bands in the relaxed system, is shifted downwards by about 3 meV by imposing the ideal geometry. As a consequence, it mixes with bulk states and shows a deeper penetration profile. The rocking mode is characterized by a stronger localization in the ideal structure compared to the relaxed surface. Also apart from the zone center we are able to identify this phonon with an energy of 8.42 meV at the $\overline{X}$ point and 7.74 meV at the $\overline{X'}$ point.

VI. CONCLUSIONS

We have reported on the results of an *ab initio* calculation of the complete phonon dispersion of bulk InP and of the InP(110) surface. The bulk phonon dispersion has been determined in good agreement with the experimental data from inelastic neutron scattering[11] and Raman spectroscopy.[12,13] Because of the large mass mismatch between indium and phosphorus, the acoustical and optical phonons are separated by a wide gap. Particularly, our calculations predict an additional gap between the transverse optic and longitudinal optic bulk bands, due to the flatness of the optic branches.

In a completely self-consistent way, we have extended our *ab initio* calculations to a system of periodically repeated thin crystal films, in order to investigate the atomic geometry and the phonon dispersion of the InP(110) surface. By relaxing the atomic positions with the help of the Hellmann-Feynman forces, we have determined the atomic equilibrium structure of the surface in good accordance with LEED measurements[21–23,27] and low-energy positron diffraction.[27] We have calculated the full phonon dispersion of InP(110) in the direction of the surface chains ($\overline{\Gamma X}$ direction) and in the direction perpendicular to the In-P chains ($\overline{\Gamma X'}$ direction). The surface-localized phonon modes identified in our calculations compare very well with the phonon dispersion experimentally determined by HREELS.[18] Especially, we find that the energy loss measured by HREELS at about 33 meV in the gap region of the bulk originates in two surface-localized phonon modes lying close together side by side.

The use of additionally constructed pseudopotentials in our density-functional calculations has confirmed the reliability of our results. Particular attention has been focused on the dependence of the surface vibrational features on the structural details of InP(110). Each of the two phonon modes at about 33 meV appears to be very sensitive even to only small variations in the atomic surface geometry. Beside the investigation of the dynamics

in the relaxed system, we have performed additional calculations for the ideal surface. In contrast with the good agreement between the experimental data and our results for the phonon dynamics determined for the relaxed surface, we observe drastic changes in the frequencies of the gap modes and the three acoustic branches in the $\overline{\Gamma X'}$ direction by removing artificially the surface relaxation. Therefore, the energy loss seen by HREELS in the gap region of the bulk phonons and the acoustic surface vibration experimentally resolved at about 7 meV in the near of the $\overline{X'}$ point can unambiguously be identified to be real fingerprints of the atomic structure of the InP(110) surface.

ACKNOWLEDGMENTS

We are indebted to S. Baroni and P. Giannozzi as well as to W. Windl for providing numerical support. We thank H. Nienhaus and W. Mönch for providing their experimental data. Our calculations have been accomplished by using the Cray-YMP supercomputers of the HLRZ of the KFA in Jülich under Contract No. K2710000 and the Leibniz Rechenzentrum in München. This work has been supported by a grant of the *Deutsche Forschungsgemeinschaft* through the Graduiertenkolleg *"Komplexität in Festkörpern: Phononen, Elektronen und Strukturen."*

[1] S. Baroni, P. Giannozzi, and A. Testa, Phys. Rev. Lett. **58**, 1861 (1987).
[2] P. Giannozzi, S. de Gironcoli, P. Pavone, and S. Baroni, Phys. Rev. B **43**, 7231 (1991).
[3] J. Fritsch, P. Pavone, and U. Schröder, Phys. Rev. Lett. **71**, 4194 (1993).
[4] U. Harten and J. P. Toennies, Europhys. Lett. **4**, 833 (1987).
[5] R. B. Doak and D. B. Nguyen, J. Electron. Spectrosc. Relat. Phenom. **44**, 205 (1987).
[6] H. Nienhaus and W. Mönch, Phys. Rev. B **50**, 11 750 (1994).
[7] J. Q. Wang, Z. Q. Gu, and M. F. Li, Phys. Lett. A **155**, 506 (1991).
[8] A. Umerski and G. P. Srivastava, Phys. Rev. B **51**, 2334 (1995).
[9] J. L. A. Alves, J. Hebenstreit, and M. Scheffler, Phys. Rev. B **44**, 6188 (1991).
[10] N. Marzari, S. de Gironcoli, and S. Baroni, Phys. Rev. Lett. **72**, 4001 (1994).
[11] P. H. Borcherds, G. F. Alfrey, D. H. Saunderson, and A. D. B. Woods, J. Phys. C **8**, 2022 (1975).
[12] R. Trommer, H. Müller, and M. Cardona, Phys. Rev. B **31**, 4896 (1980).
[13] A. Mooradian and G. B. Wright, Solid State Commun. **4**, 431 (1966).
[14] P. H. Borcherds and K. Kunc, J. Phys. C **11**, 4145 (1978).
[15] M. S. Kushwaha and S. S. Kushwaha, Can. J. Phys. **58**, 351 (1980).
[16] H. -M. Kagaya and T. Soma, Phys. Status Solidi **121**, K113 (1984).
[17] G. K. Schenter and J. P. LaFemina, J. Vac. Sci. Technol. A **10**, 2429 (1992).
[18] H. Nienhaus and W. Mönch, Surf. Sci. **328**, L561 (1995).
[19] P. K. Das and R. E. Allen, *Physics of Semiconductors: Proceedings of the 20th International Conference*, edited by E. M. Anastassakis and J. D. Joannopoulos (World Scientific, Singapore, 1990), p. 1473.
[20] Y. R. Wang and C. B. Duke, Surf. Sci. **205**, L755 (1988).
[21] W. K. Ford, T. Guo, K. -J. Wan, and C. B. Duke, Phys. Rev. B **45**, 11 896 (1992).
[22] C. B. Duke, A. Paton, C. Mailhiot, and A. Kahn, J. Vac. Sci. Technol. B **3**, 1087 (1985).
[23] R. J. Meyer, C. B. Duke, A. Paton, J. C. Tsang, J. L. Yeh, A. Kahn, and P. Mark, Phys. Rev. B **22**, 6171 (1980).
[24] J. C. Woicik, T. Kendelewicz, K. E. Miyano, P. L. Cowan, C. E. Bouldin, B. A. Karlin, P. Pianetta, and W. E. Spicer, Phys. Rev. Lett. **68**, 341 (1992).
[25] J. C. Woicik, T. Kendelewicz, K. E. Miyano, P. L. Cowan, M. Richter, B. A. Karlin, C. E. Bouldin, P. Pianetta, and W. E. Spicer, J. Vac. Sci. Technol. A **10**, 2041 (1992).
[26] P. S. Mangat, S. T. Kim, K. M. Choudhary, Z. Hurych, and P. Soukiassian, Surf. Sci. **285**, 102 (1993).
[27] X. M. Chen, K. F. Canter, C. B. Duke, A. Paton, D. L. Lessor, and W. K. Ford, Phys. Rev. B **48**, 2400 (1993).
[28] C. B. Duke, J. Vac. Sci. Technol. A **10**, 2032 (1992).
[29] C. Mailhiot, C. B. Duke, and D. J. Chadi, Surf. Sci. **149**, 366 (1985).
[30] P. Hohenberg and W. Kohn, Phys. Rev. **136**, B864 (1964).
[31] W. Kohn and L. J. Sham, Phys. Rev. **140**, A1133 (1965).
[32] D. M. Ceperley and B. I. Alder, Phys. Rev. Lett. **45**, 566 (1980).
[33] J. Perdew and A. Zunger, Phys. Rev. B **23**, 5048 (1981).
[34] T. Pletl (private communication). The pseudopotentials have been generated using for the s and p states the electronic ground-state configuration and the ionized configurations $3s^2 3p^{2.5} 3d^{0.25}$ for P and $5s^{1.75} 5p^{0.25} 5d^{0.75}$ for In. The core radii are $r_c^s = 1.7$, $r_c^p = 1.8$, and $r_c^d = 2.0$ for P, and $r_c^s = 2.4$, $r_c^p = 3.1$, and $r_c^d = 4.2$ for In.
[35] N. Troullier and J. L. Martins, Phys. Rev. B **43**, 1993 (1991).
[36] F. D. Murnaghan, Proc. Natl. Acad. Sci. U.S.A. **50**, 697 (1944).
[37] The numbers (LMN) define a set of points $\mathbf{q}_{lmn} = \frac{l}{\mathrm{L}}\mathbf{G}_1 + \frac{m}{\mathrm{M}}\mathbf{G}_2 + \frac{n}{\mathrm{N}}\mathbf{G}_3$ with $0 \leq l \leq \mathrm{L}-1$, $0 \leq m \leq \mathrm{M}-1$, and $0 \leq n \leq \mathrm{N}-1$. The vectors $\mathbf{G}_1$, $\mathbf{G}_2$, and $\mathbf{G}_3$ are the primitive translations of the reciprocal space of a fcc lattice.
[38] *Semiconductors: Physics of Group IV and III-V Compounds*, edited by O. Madelung, Landolt-Börnstein, New Series, Group 3, Vol. 17, Pt. a (Springer-Verlag, Berlin, 1982); *Semiconductors: Intrinsic Properties of Group IV Elements and III-V, II-VI, and I-VII Compounds*, edited by O. Madelung, Landolt-Börnstein, New Series, Group 3, Vol. 22, Pt. a (Springer-Verlag, Berlin, 1987).
[39] D. Vanderbilt and S. G. Louie, Phys. Rev. B **30**, 6118 (1984).
[40] R. Di Felice, A. I. Shkrebtii, F. Finocchi, C. M. Bertoni, and G. Onida, J. Electron. Spectrosc. Relat. Phenom. **64/65**, 697 (1993).
[41] J. A. Schaefer, Surf. Sci. **178**, 90 (1986).
[42] L. H. Dubois and G. P. Schwartz, Phys. Rev. B **26**, 794 (1982).